Inflammation (© 2018)
DOI: 10.1007/s10753-018-0812-9

ORIGINAL ARTICLE

Andrographolide Ameliorates Atherosclerosis by Suppressing Pro-Inflammation and ROS Generation-Mediated Foam Cell Formation

Teng Wu,[1,2] Yuan Peng,[1,3] Sishan Yan,[4] Ning Li,[4] Yinghua Chen,[5,7] and Tian Lan[4,6,7]

Abstract—Inflammation, oxidative stress, and dyslipidemia are major factors in the pathogenesis of atherosclerosis. Andrographolide, a bioactive component of *Andrographis paniculata*, has several biological activities, including anti-inflammatory, antioxidant, and anticancer effects. This study shows that andrographolide downregulates the oxidized low-density lipoprotein (oxLDL)-induced expression of the pro-inflammatory molecules monocyte chemotactic protein (MCP)-1 and interleukin (IL)-6 and blocks the nuclear factor-κB signaling pathway in macrophages. Additionally, andrographolide treatment decreased reactive oxygen species (ROS) generation in oxLDL-induced macrophages, indicating that the compound can decrease oxidative stress. The results also suggest that andrographolide suppresses oxLDL-induced foam cell formation and inhibits oxLDL-induced CD36 expression *in vitro*. Furthermore, *in vivo* studies have indicated that andrographolide treatment ameliorates atherosclerosis pathogenesis in apolipoprotein E knockout mice. Therefore, by suppressing inflammation, ROS generation, and foam cell formation, andrographolide may ameliorate the progression of atherosclerosis, suggesting its potential as a therapeutic drug for the prevention and/or treatment of this disease.

KEY WORDS: andrographolide; atherosclerosis; inflammation; reactive oxygen species; foam cell formation.

INTRODUCTION

Atherosclerosis is a chronic inflammatory disease that affects a large number of people worldwide. The condition is associated with various complications, such as angina pectoris, hypertension, and limb ischemia [1, 2]. Currently, the main therapeutic strategy for atherosclerosis is regulation of lipid metabolism to slow the progression of the disease rather

Teng Wu and Yuan Peng contributed equally to this work.

[1] Center of Biomedical Engineering, Zhongshan School of Medicine, Sun Yat-sen University, Guangzhou, 510080, China
[2] Key Laboratory of Cardiovascular Disease and Department of Pathophysiology, Nanjing Medical University, Nanjing, Jiangsu, China
[3] Department of Rehabilitation Medicine, Guangzhou First People's Hospital, Second Affiliated Hospital of South China University of Technology, Guangzhou, Guangdong, China
[4] School of Pharmacy, Guangdong Pharmaceutical University, Guangzhou, 510006, China
[5] Organ Transplantation Center, The First Affiliated Hospital, Sun Yat-sen University, 58 Zhongshan 2nd Rd, Guangzhou, 510080, China
[6] Department of Pharmacology, School of Pharmacy, Guangdong Pharmaceutical University, Guangzhou Higher Education Mega Center, 280 Wai Huan Dong Road, Guangzhou, 510006, China
[7] To whom correspondence should be addressed to Yinghua Chen at Organ Transplantation Center, The First Affiliated Hospital, Sun Yat-sen University, 58 Zhongshan 2nd Rd, Guangzhou, 510080, China. E-mail: chyh9@mail.sysu.edu.cn; and Tian Lan at Department of Pharmacology, School of Pharmacy, Guangdong Pharmaceutical University, Guangzhou Higher Education Mega Center, 280 Wai Huan Dong Road, Guangzhou, 510006, China. E-mail: lantian012345@163.com

Published online: 14 June 2018

than decrease plaques. Statins, which are lipid-lowering medications, are the most commonly prescribed treatment for atherosclerosis, being used by millions of patients. However, the adverse effects associated with statins, such as myopathy and diabetes mellitus, limit their usage [3].

Macrophages participate in all atherosclerosis-related processes, including the initiation, progression, and regression of atherosclerotic lesions [4]. Endothelial dysfunction and structural alterations cause the accumulation of low-density lipoproteins (LDL) in the subendothelial space, leading to atherogenesis [5, 6]. Once LDLs are retained in the intima, they are prone to be oxidized by reactive oxygen species (ROS) [7, 8], causing the formation of oxidized LDL (oxLDL). This, in turn, triggers the expression of monocyte chemotactic protein (MCP)-1 and the release of several cytokines, such as interleukin (IL)-6 and tumor necrosis factor (TNF)-α, promoting the recruitment of monocytes, which subsequently differentiate into macrophages [9]. These macrophages internalize oxLDL through the scavenger receptors CD36 and ScR-A, gradually becoming foam cells [10]. The apoptosis of foam cells releases their lipid contents, leading to further inflammation and, eventually, the development of atherosclerotic plaques [11]. Together, dyslipidemia, inflammation, and oxidative stress play a significant role in the pathogenesis of atherosclerosis.

Andrographolide, a labdane diterpenoid, is a natural compound isolated from *Andrographis paniculata*. A traditional Chinese medicine, andrographolide has been officially approved for the treatment of respiratory infections and fever. Recently, andrographolide has been found to exert strong anti-inflammatory activity by blocking the nuclear factor (NF)-κB signaling pathway [12]. Additional studies have highlighted the benefits of its anti-inflammatory effects in diseases such as cancer and diabetes [13–15]. However, few studies have investigated whether andrographolide can inhibit the progression of atherosclerosis. In the present work, the anti-atherosclerotic effects of andrographolide are examined, and data are provided showing that andrographolide significantly ameliorates the dyslipidemia, inflammation, and oxidative stress induced by oxLDL in macrophages and alleviates the progression of atherosclerosis.

MATERIALS AND METHODS

Reagents

Andrographolide and dimethyl sulfoxide (DMSO) were purchased from Sigma Aldrich (St. Louis, MO, USA). The 3-(4,5-dimethylthiazol-2-yl)-2,5-diphenyl tetrazolium bromide (MTT) Cell Proliferation and Cytotoxicity Assay kit was obtained from Sangon (Shanghai, China). Primary antibodies against p65 and phosphorylated (p)-p65 were purchased from Santa Cruz Biotechnology. Primary antibodies against CD36 were obtained from Abcam, and primary antibodies against β-actin were from Beyotime Biotechnology Co. (Beijing, China).

Cell Culture and Treatment

The murine macrophage cell line RAW264.7 was provided by the American Type Culture Collection (Manassas, VA, USA). RAW264.7 cells were cultured at 37 °C in a 5% CO_2 incubator with Dulbecco's modified Eagle's medium (DMEM; Gibco, USA) containing 10% fetal bovine serum (Gibco, USA) and 100 U/mL penicillin-streptomycin. Cells were grown to confluence and synchronized in serum-free DMEM for 12 h. The medium was then changed to (1) serum-free DMEM for 48 h (negative control), (2) serum-free DMEM with 80 μg/mL oxLDL (Yiyuan, Guangzhou, China) for 48 h, (3) oxLDL-containing serum-free DMEM with 1 μM andrographolide for 48 h, (4) oxLDL-containing serum-free DMEM with 5 μM andrographolide for 48 h, or (5) oxLDL-containing serum-free DMEM with 100 μM PDTC for 48 h.

MTT Assay

RAW264.7 cells were seeded in 96-well plates at 4×10^3 cells/well; at 60% confluence, the cells were starved for 3 h and then incubated with different concentrations of andrographolide (0, 1.25, 2.5, 5, 10, 20, and 40 μM) in DMEM for 48 h. MTT (1%, 10 μL) was then added to each well, followed by incubation for 2–4 h. The medium was then carefully removed, and 100 μL DMSO was added to each well. The absorbance of solubilized blue formazan was read at 490 nm by using a microplate reader.

RNA Extraction and Real-time Polymerase Chain Reaction

RNA was extracted by using TRIzol (Invitrogen) according to the manufacturer's recommended protocol. A reverse transcription kit (Takara) and oligo(dT) primers were used for the reverse transcription. cDNA was amplified and measured by using a StepOnePlus system (Applied Biosystems). The quantitative (q)PCR primer sequences were as follows: IL-6, forward 5′-TAGTCCTT CCTACCCCAATTTCC-3′ and reverse 5′-TTGGTCCT

TAGCCACTCCTTC-3′; MCP-1, forward 5′-TTAA AAACCTGGATCGGAACCAA-3′ and reverse 5′-GCAT TAGCTTCAGATTTACGGGT-3′; and CD36, forward 5′-ATGGGCTGTGATCGGAACTG-3′ and reverse 5′-GTCT TCCCAATAAGCATGTCTCC-3′. PCR primers for β-actin were purchased from Sangon. Quantitative measurements were obtained by using the ΔCt method, with β-actin as an internal control.

MCP-1 and IL-6 Detection

RAW264.7 cells were treated as described above. Brefeldin A (10 μg/mL) was added to each well 8 h before harvest. BD Fc BlockTM (100 μL/well) was then added, followed by incubation for 30 min at 4 °C to block non-specific antibody binding sites. After thrice washing with washing buffer, a permeabilization solution (100 μL/well) was added, followed by incubation for 20 min at 4 °C. The cells were then incubated with Alexa Fluor 488-conjugated anti-mouse IL-6 (BD, USA) and PE-conjugated anti-mouse MCP-1 (BD, USA) for 30 min at 4 °C, washed thrice, and analyzed on a CytoFLEX flow cytometer by using the CytExpert software (Beckman, USA).

Western Blot Analysis

Total cellular proteins were extracted from RAW264.7 cells by using RIPA Lysis Buffer (Beyotime, Shanghai, China) according to the manufacturer's protocol. Protein samples (30 μg) were separated by using 12% sodium dodecyl sulfate–polyacrylamide gel electrophoresis and then transferred to polyvinylidene difluoride membranes. The membranes were incubated for 1 h with a blocking buffer (5% nonfat milk dissolved in Tris-buffered saline containing 0.1% Tween 20 (TBST)) and then overnight at 4 °C with mouse antibodies against β-actin (for normalization of protein expression), rabbit antibodies against p-p65, rabbit antibodies against CD36, or mouse antibodies against p65. Horseradish peroxidase (HRP)-conjugated donkey anti-mouse or anti-rabbit IgG (Santa Cruz Biotechnology) was used to amplify the immunogenic signals. Protein signals were detected on a LAS 4000 imaging system (GE, USA) by using a chemiluminescence kit (KeyGen, Nanjing, China).

Evaluation of Cellular ROS Levels

Cells were plated in glass-bottom cell culture dishes at 8×10^3 cells/dish and incubated overnight. After the treatments described in the "Cell Culture and Treatment" section, dichlorofluorescin diacetate (DCFH-DA; 10 μM) was added to each dish, followed by incubation for another 90 min. Subsequently, the dishes were washed thrice with phosphate-buffered saline (PBS), fixed with 4% paraformaldehyde for 5 min, and stained with 4′,6-diamidino-2-phenylindole (DAPI) for 1 min. The samples were then observed under a confocal microscope (Zeiss 710, Germany).

Measurement of Macrophage Uptake

Cells were seeded on cover glasses in 6-well plates (8×10^3 cells/well) and, after serum starvation overnight, were treated as described in the "Cell Culture and Treatment" section. Then, 40 μg/mL Dil-labeled oxLDL (Yiyuan, Guangzhou, China) was added to all samples except those in the control group, followed by incubation for 3 h. After treatment, the cells were washed thrice with PBS, fixed with 4% paraformaldehyde for 5 min, and stained with DAPI for 2 min. The cells were then observed by using confocal microscopy.

Animal Feeding and Treatment

Homozygous apolipoprotein E-deficient ($ApoE^{-/-}$) mice were obtained from the Jackson Laboratory. The mice were housed under a fixed 10:14-h light/dark cycle and treated according to the guidelines of the Animal Experimental Center of Guangdong Pharmaceutical University. The $ApoE^{-/-}$ mice were fed with a Western diet for 8 weeks and then separated into three groups with similar body weights. The groups were intraperitoneally injected with 1 μg/g andrographolide, 2.5 μg/g andrographolide, and PBS, respectively, every 3 days for an additional 8 weeks.

Measurement of Atherosclerotic Lesions

Mice were sacrificed by using an overdose of ethyl ether and then perfused with PBS. To assess the development of atherosclerosis, both aortic root sections and the thoracic/abdominal aortas that separated from fat or other tissues were stained with Oil Red O (Sangon, Shanghai, China) for 30 min. The Image Pro Plus 6.0 imaging software was used to measure aortic lesions by using the "en face" method as previously described [10].

Immunohistochemistry

For immunohistochemistry, aortic root sections were incubated with rat anti-MCP-1 (1:100; Abcam) and rabbit anti-IL-6 antibodies (1:100; Abcam) at 4 °C overnight and then with goat anti-rabbit or anti-rat

secondary antibodies (Santa Cruz Biotechnology, USA) at 37 °C for at least 1 h. The protein expression was visualized by using 3,3′-diaminobenzidine (Thermo) for 1.5 min; hematoxylin was used to stain the nuclei.

Statistical Analysis

Significant differences between two groups were analyzed by using the unpaired Student's *t* test, and differences among multiple groups were assessed by applying one-way analysis of variance with Bonferroni's correction (GraphPad Prism software version 5.0; GraphPad Prism, USA). All experiments were done at least in triplicate, with similar results. The data are expressed as the mean ± standard deviation (SD). Statistical significance was set to $P < 0.05$.

RESULTS

Andrographolide Inhibits oxLDL-Induced Inflammation in RAW264.7 Cells

To determine the appropriate andrographolide concentration for use with RAW264.7 cells, the cells were exposed to 0–40 μM andrographolide for 48 h. As shown in Fig. 1a, the viability of RAW264.7 cells was not altered by andrographolide at a concentration lower than 10 μM (91.3% ± 4.4). Thus, in the following experiments, RAW264.7 cells were cultured with 1 or 5 μM andrographolide.

The increased expression of pro-inflammatory cytokines, such as MCP-1 and IL-6, is considered one of the hallmarks of atherosclerosis [16]. The data shown in Fig. 1b indicate that the *MCP-1* mRNA levels significantly

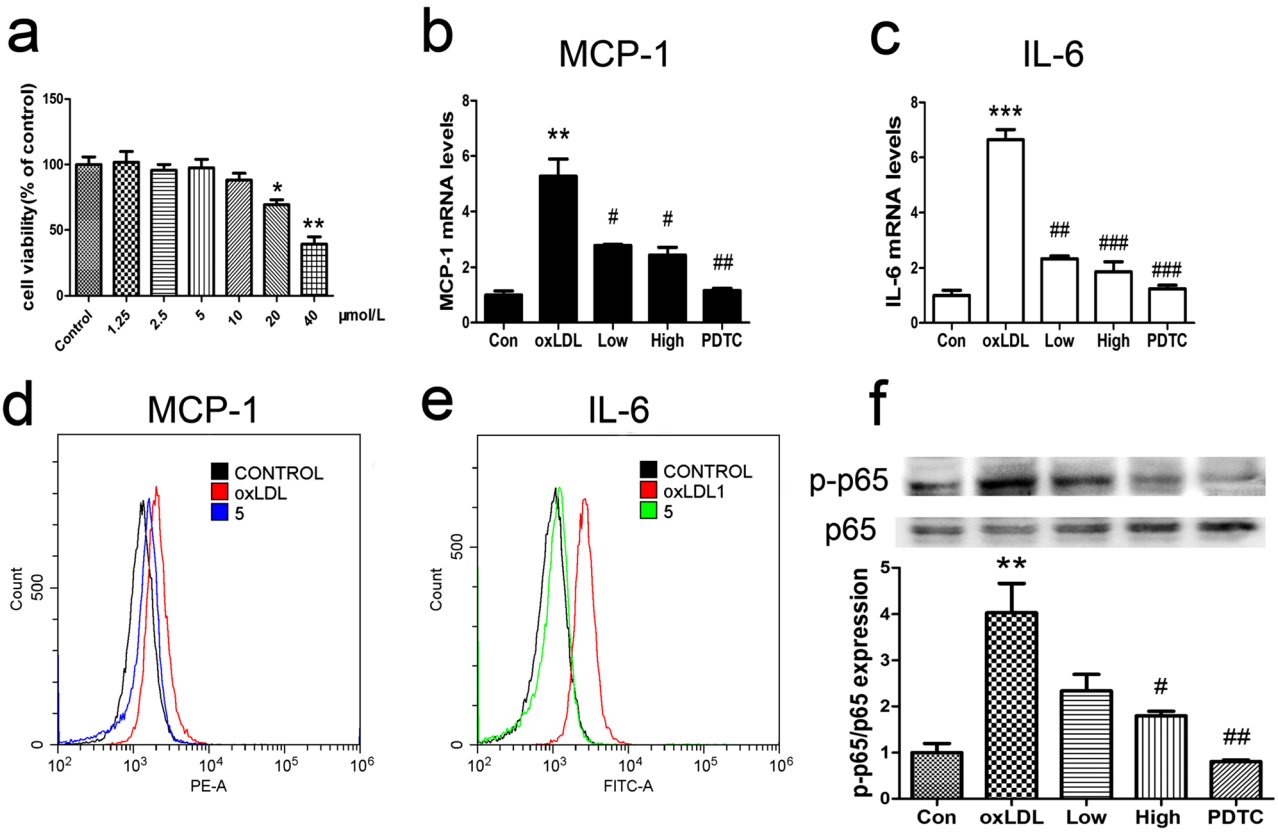

Fig. 1. Anti-inflammatory efficacy of andrographolide on oxLDL-induced macrophages. **a** Cytotoxicity in RAW264.7 cells treated with different concentrations of andrographolide. mRNA levels of **b** MCP-1 and **c** IL-6 in RAW264.7 cells treated with 1 and 5 μM andrographolide in the presence of oxLDL (80 μg/mL) for 24 h. **d** MCP-1 and **e** IL-6 protein expression in RAW264.7 cells treated with 5 μM andrographolide in the presence of oxLDL (80 μg/mL) as measured by flow cytometry. **f** P-p65 levels in RAW264.7 cells treated with 1 and 5 μM andrographolide in the presence of oxLDL (80 μg/mL). All experiments were done at least in triplicate. PDTC was used as a positive control. $*P < 0.05$, $**P < 0.01$, and $***P < 0.001$ *vs.* control group. $\#\#P < 0.01$ and $\#\#\#P < 0.001$ *vs.* oxLDL treatment group.

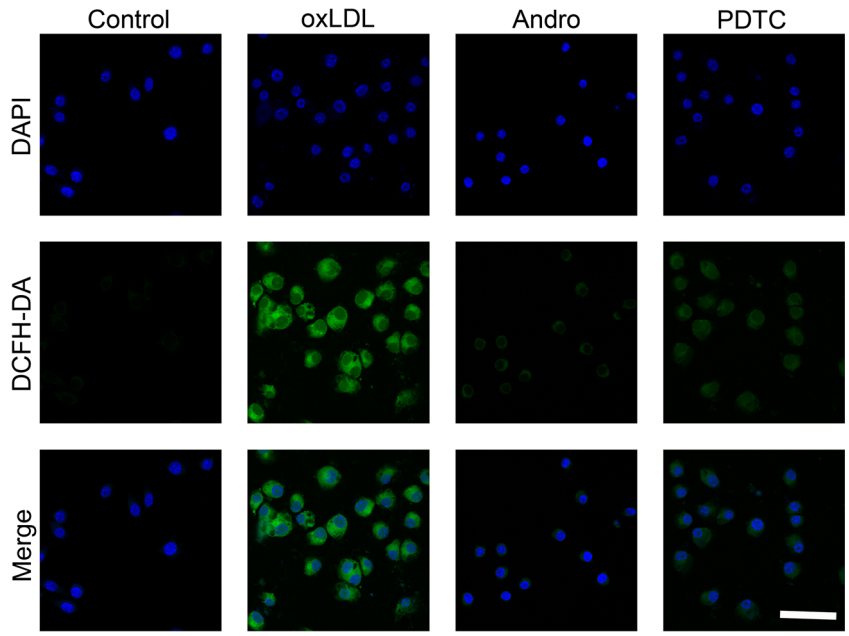

Fig. 2. Andrographolide decreases ROS generation in oxLDL-induced macrophages. ROS levels in RAW264.7 cells treated with 5 μM andrographolide in the presence of oxLDL (80 μg/mL) were visualized by confocal microscopy (bar, 50 μm). All experiments were done at least in triplicate.

increased (up to 5.28 ± 0.67-fold) on oxLDL treatment. However, in cells treated with oxLDL, andrographolide decreased the *MCP-1* transcription (2.77 ± 0.11- and 2.43 ± 0.31-fold that of control after treatment with 1 and 5 μM andrographolide, respectively); this effect is similar to that of the NF-κB inhibitor PDTC (1.16 ± 0.12 compared with control). Additionally, andrographolide inhibited the *IL-6* transcription in oxLDL-stimulated macrophages (Fig. 1c): 1 and 5 μM andrographolide significantly decreased the *IL-6* levels in oxLDL-stimulated macrophages (2.33 ± 0.09- and 1.86 ± 0.30-fold that of control, respectively) compared with the oxLDL-treated group (6.64 ± 0.41-fold that of control). Flow cytometry was used to evaluate the MCP-1 and IL-6 protein levels in the same conditions. As shown in Fig. 1d, e, similarly to PDTC, andrographolide (5 μM) decreased the MCP-1 and IL-6 expression in oxLDL-induced macrophages.

Andrographolide Hampers the oxLDL-Induced Activation of NF-κB Signaling in RAW264.7 Cells

The activation of the inflammatory response-related NF-κB signaling pathway plays an important role in the progression of atherosclerosis. The data reported above indicate that andrographolide has a similar effect to that of PDTC, a selective NF-κB inhibitor. The phosphorylation of p65 is important for NF-κB activation [17]. Therefore, to investigate if andrographolide activated NF-κB signaling, the p65 phosphorylation was measured by Western blot assays. A marked increase in p65 phosphorylation after oxLDL treatment (4.03 ± 0.76-fold that of control) was observed, whereas andrographolide treatment (1 and 5 μM) decreased the p-p65 levels in a dose-dependent manner (2.34 ± 0.40- and 1.79 ± 0.21-fold that of control at 1 and 5 μM, respectively; Fig. 1f). These results are similar to those obtained with PDTC treatment (0.83 ± 0.10-fold that of control; Fig. 1f).

Andrographolide Treatment Inhibits oxLDL-Induced ROS Generation in Macrophages

Next, DCFH-DA, a fluorogenic ROS dye, was used to evaluate oxidative stress in oxLDL-treated cells. As shown in Fig. 2, the DCFH-DA fluorescence was much stronger in oxLDL-induced macrophages than in negative control cells, indicating ROS generation after oxLDL treatment. Andrographolide treatment weakened the fluorescence of oxLDL-treated cells, indicating decreased ROS production on andrographolide treatment; PDTC had only a slight effect on the level of oxidative stress in oxLDL-treated cells.

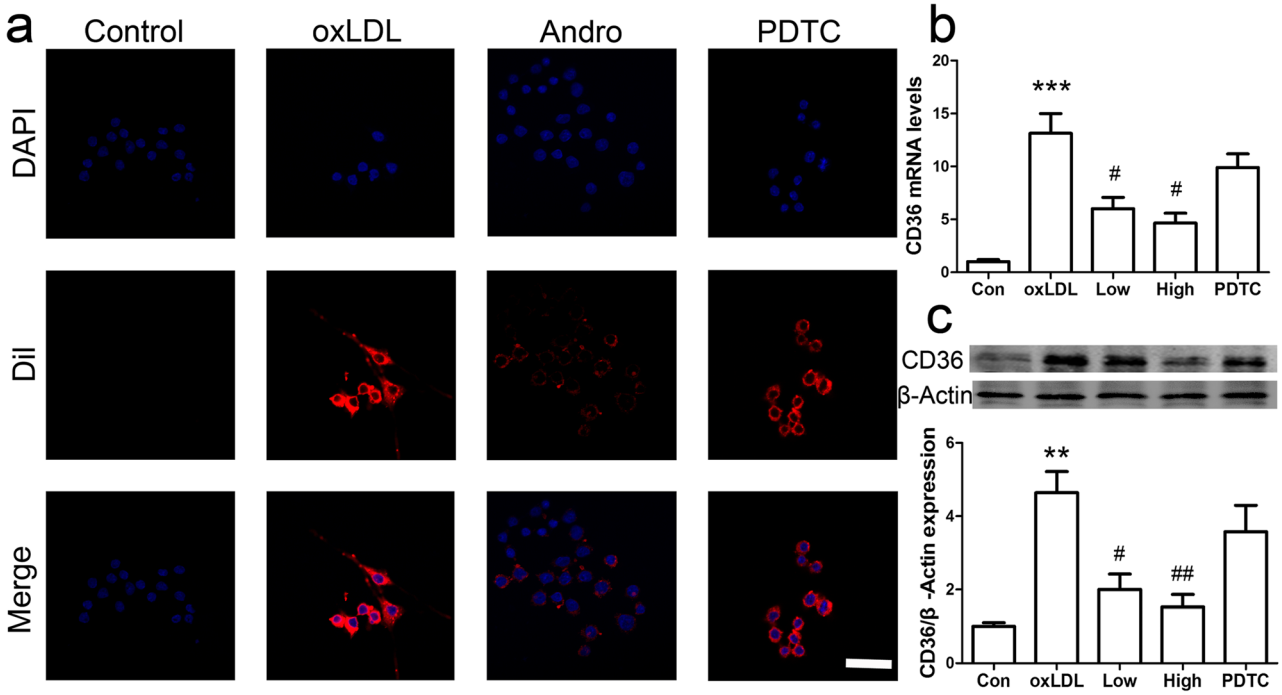

Fig. 3. Andrographolide blocks oxLDL-induced foam cell formation and CD36 upregulation. **a** RAW264.7 cells were treated with 5 μM andrographolide in the presence of Dil-labeled oxLDL (40 μg/mL). The Dil-labeled oxLDL uptake was measured by confocal microscopy. **b** RAW264.7 cells were treated with 1 and 5 μM andrographolide in the presence of oxLDL (80 μg/mL) for 24 h. The CD36 mRNA levels were analyzed by q-PCR. **c** RAW264.7 were cells treated with 1 and 5 μM andrographolide in the presence of oxLDL (80 μg/mL) for 48 h. The CD36 expression was measured by Western blotting assays. All experiments were done at least in triplicate. Bar, 50 μm. $^{**}P < 0.01$ and $^{***}P < 0.001$ *vs.* control group. $\#P < 0.05$ and $\#\#P < 0.01$ *vs.* oxLDL treatment group.

Andrographolide Treatment Inhibits oxLDL-Induced CD36 Expression and Foam Cell Formation

Foam cell formation is key to the development of atherosclerosis, and macrophages can internalize oxLDL to form foam cells *in vitro*. Thus, Dil-labeled oxLDL was used to evaluate foam cell formation. As shown in Fig. 3a, weaker red fluorescence was observed in the andrographolide-treated group compared with the oxLDL-stimulated group, indicating that andrographolide suppressed oxLDL internalization. CD36, a class A scavenger receptor, participates in foam cell formation induced by oxLDL internalization [18]. Real-time PCR assays, shown in Fig. 3b, indicated that andrographolide treatment of oxLDL-stimulated macrophages downregulation of *CD36* mRNA levels (5.22 ± 1.32- and 4.57 ± 0.74-fold that of control on treatment with 1 and 5 μM andrographolide, respectively) compared with oxLDL-stimulated macrophages (12.9 ± 2.1-fold that of control). Similar results were obtained in Western blot assays (Fig. 3c): treatment with 1 and 5 μM andrographolide was associated with downregulated CD36 expression (2.00 ± 0.32- and 1.52 ± 0.28-fold that of control, respectively) compared with that in oxLDL-treated macrophages (4.64 ± 0.52-fold that of control). Conversely, PDTC did not have any effect on CD36 expression in oxLDL-induced macrophages (Fig. 3b, c).

Andrographolide Treatment Counteracts the Progression of Atherosclerosis

ApoE$^{-/-}$ mice fed with a Western diet were used to evaluate the therapeutic effects of andrographolide *in vivo*. Oil Red O staining, which allows the visualization of lipids, showed plaque reduction in the aortic roots (Fig. 4a, b) and aortic trees (Fig. 4c, d) after andrographolide treatment, indicating that andrographolide dose-dependently counteracts the progression of atherosclerosis. Immunohistochemistry assays, which evaluated the MCP-1 and IL-6 levels in plaques from each group, showed that the expression of MCP-1 (Fig. 4e, f) and IL-6 (Fig. 4g, h) was downregulated in plaques after andrographolide treatment. Interestingly, these results also indicated the dose-dependent effect of andrographolide in decreasing atherosclerotic

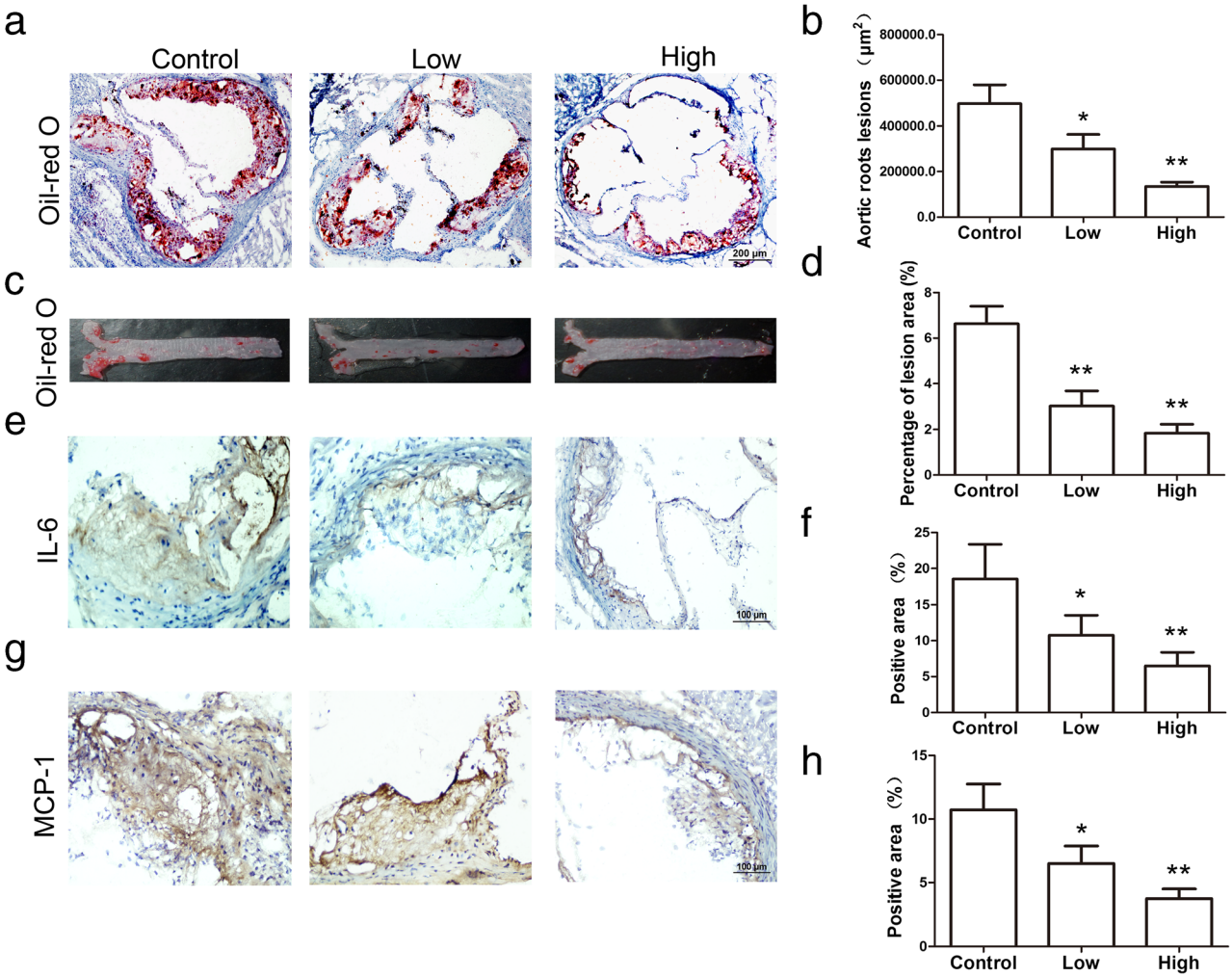

Fig. 4. Protective effects of andrographolide on atherosclerosis in ApoE$^{-/-}$ mice. ApoE$^{-/-}$ mice fed with a Western diet were intraperitoneally injected with 1 or 2.5 μg/g andrographolide every 3 days for 8 weeks. The plaques in the aortic root (**a** and **b**) and aortic tree (**c** and **d**) were analyzed by Oil red O staining and quantified by using the ImageJ software, respectively. The expression of IL-6 (**e** and **f**) and MCP-1 (**g** and **h**) in the aortic roots was examined by immunohistochemical staining and quantified by using the ImageJ software. Bar, 200 μm in Oil Red O staining images and 100 μm in immunohistochemistry staining images ($n = 8$ per group; $^*P < 0.05$ and $^{**}P < 0.01$ *vs* control group).

plaques, as well as in inhibiting the expression of the pro-inflammatory factors MCP-1 and IL-6.

DISCUSSION

Despite some effective therapeutic strategies in clinical practice, atherosclerosis is still the leading cause of mortality and morbidity in developed countries. In this preclinical study, andrographolide was found to alleviate the progression of atherosclerosis.

Andrographis (*Andrographis paniculata*), a traditional Chinese medicine, shows several pharmacologic effects, including anti-inflammatory, immunoregulatory, anticancer, and hypoglycemic activities [19]. For over a decade now, andrographolide, extracted from Andrographis, has been recognized as an anti-inflammatory compound both *in vivo* and *in vitro*. For instance, it can inhibit NF-κB activation and attenuate neointimal hyperplasia in arterial restenosis [12]. A recent study reported that andrographolide treatment inhibits the production of NO and TNF-α in lipopolysaccharide (LPS)-treated peritoneal mouse macrophages. However, although treatment with andrographolide in combination with LPS decreases IL-6 production, the decrease is not significant compared with treatment with LPS alone [20], indicating the complex role IL-6 plays in inflammation. IL-6

has been described as anti-inflammatory in some settings, and some studies have reported that classical IL-6 signaling is initialed through the binding of IL-6 to the non-signaling IL-6 receptor α (IL-6Rα) subunit, which promotes IL-6-mediated inflammation response [21, 22]. However, in some leukocytes, the expression of the IL-6Rα subunit is restricted, limiting the types of cells that respond to IL-6 [21, 22]. Nevertheless, many studies have suggested that IL-6 also plays essential roles in promoting inflammation and immune system activation. For example, several works have confirmed that andrographolide treatment significantly decreases IL-6 expression in LPS-activated RAW264.7 cells and in acute lung injury [23, 24]; andrographolide treatment also inhibits macrophage activation in adjuvant-induced arthritis [20]. These varying observations regarding IL-6 expression on andrographolide treatment are probably due to the different types of macrophages used in the studies. The present research found that in oxLDL-induced RAW264.7 cells treated with andrographolide, the expression of the pro-inflammatory factors IL-6 and MCP-1 decreased, and p65 phosphorylation, which plays an important role in NF-κB activation, was inhibited.

ROS are generated in nearly all cell types, and they function as signaling molecules in various metabolic processes [25]. Several studies have indicated the role of ROS in the pathogenesis of atherosclerosis, and decreasing ROS levels is a useful strategy for the treatment of this disease [26]. Andrographolide has been reported to ameliorate diabetic nephropathy by attenuating hyperglycemia-mediated renal oxidative stress and inflammation through the Akt/NF-κB pathway [13]. Here, andrographolide treatment was found to be associated with the decreased ROS generation in oxLDL-induced macrophages, indicating that andrographolide ameliorates oxidative stress in oxLDL-treated cells.

Foam cell formation is one of the most important events in atherosclerotic progression [10]. The conversion of macrophages into foam cells is synergized by imbalances in the normal homeostatic mechanisms that control the binding and uptake, intracellular metabolism, and efflux of cholesterol [27]. Lipoprotein uptake by monocyte-derived macrophages is one of the earliest pathogenic events in atherosclerosis and results in the development of foam cells. Scavenger receptors, a type of pattern recognition receptors expressed by macrophages, play a key role in atherosclerosis [28]. Numerous scavenger receptor family members promote foam cell formation. Among them, scavenger receptor A1 (SR-A1) and CD36 mediate 75–90% of the modified LDL degradation by macrophages *in vitro* [29]. In this study, the CD36 expression and oxLDL uptake in oxLDL-induced macrophages were evaluated, and andrographolide treatment was found to inhibit oxLDL-induced CD36 expression and block foam cell formation *in vitro*. The ATP-binding cassette (ABC) subfamily members ABCA1 and ABCG1 mediate cholesterol efflux in foam cells. Lin et al. showed that andrographolide treatment inhibits foam cell formation in macrophages by inhibiting CD36-mediated oxLDL uptake and inducing ABCA1- and ABCG1-dependent cholesterol efflux [30], providing a mechanism for andrographolide-mediated foam cell formation. Further research on this subject also evaluated the therapeutic effects of andrographolide on $ApoE^{-/-}$ mice fed with a Western diet. The present results showed that andrographolide dose-dependently decreased the expression of IL-6 and MCP-1 in the aortas and ameliorated the progression of atherosclerosis in $ApoE^{-/-}$ mice.

In conclusion, andrographolide was found to ameliorate oxLDL-induced oxidative stress, downregulate the expression of inflammatory factors, such as IL-6 and MCP-1, and inhibit foam cell formation *in vitro*. The results suggest that the anti-inflammatory activity of andrographolide is exerted through inhibition of the NF-κB signaling pathway. Furthermore, the *in vivo* experiments showed that andrographolide treatment decreases plaque lesions and inhibits the expression of the pro-inflammatory factors IL-6 and MCP-1 in the plaque areas in a dose-dependent manner. Therefore, the findings provide new insights into the beneficial therapeutic effects of andrographolide in the treatment of atherosclerosis.

ACKNOWLEDGMENTS

The authors thank Editage [www.editage.cn] for the English language editing. We also thank Dr. Ying Liu from Guangdong Pharmaceutical University for providing good suggestion to experimental design and supporting parts of this project.

FUNDING INFORMATION

This work was supported by science and technology development grants from Nanjing Medical University (grant no. 2017NJMU012).;the Science and Technology Planning Project of Guangdong Province (2017A020211007), China; the Key Project of Natural Science Foundation of

Guangdong Province (2016A030311014), China and the Natural Science Foundation of Guangdong Province (2015A030313582), China.

COMPLIANCE WITH ETHICAL STANDARDS

Conflict of Interest. The authors declare that they have are no conflicts of interest.

REFERENCES

1. Falk, E., M. Nakano, J.F. Bentzon, A.V. Finn, and R. Virmani. 2013. Update on acute coronary syndromes: the pathologists' view. *European Heart Journal* 34: 719–728.
2. Ouriel, K. 2001. Peripheral arterial disease. *Lancet* 358: 1257–1264.
3. Collins, R., C. Reith, J. Emberson, J. Armitage, C. Baigent, L. Blackwell, R. Blumenthal, J. Danesh, G.D. Smith, D. DeMets, S. Evans, M. Law, S. MacMahon, S. Martin, B. Neal, N. Poulter, D. Preiss, P. Ridker, I. Roberts, A. Rodgers, P. Sandercock, K. Schulz, P. Sever, J. Simes, L. Smeeth, N. Wald, S. Yusuf, and R. Peto. 2016. Interpretation of the evidence for the efficacy and safety of statin therapy. *Lancet* 388: 2532–2561.
4. Colin, S., G. Chinetti-Gbaguidi, and B. Staels. 2014. Macrophage phenotypes in atherosclerosis. *Immunological Reviews* 262: 153–166.
5. Kwon, G.P., J.L. Schroeder, M.J. Amar, A.T. Remaley, and R.S. Balaban. 2008. Contribution of macromolecular structure to the retention of low-density lipoprotein at arterial branch points. *Circulation* 117: 2919–2927.
6. Gistera, A., and G.K. Hansson. 2017. The immunology of atherosclerosis. *Nature Reviews. Nephrology* 13: 368–380.
7. Fraley, A.E., and S. Tsimikas. 2006. Clinical applications of circulating oxidized low-density lipoprotein biomarkers in cardiovascular disease. *Current Opinion in Lipidology* 17: 502–509.
8. Siti, H.N., Y. Kamisah, and J. Kamsiah. 2015. The role of oxidative stress, antioxidants and vascular inflammation in cardiovascular disease (a review). *Vascular Pharmacology* 71: 40–56.
9. Rudijanto, A. 2007. The role of vascular smooth muscle cells on the pathogenesis of atherosclerosis. *Acta Medica Indonesiana* 39: 86–93.
10. Zheng, L., T. Wu, C. Zeng, X. Li, X. Li, D. Wen, T. Ji, T. Lan, L. Xing, J. Li, X. He, and L. Wang. 2016. SAP deficiency mitigated atherosclerotic lesions in ApoE(-/-) mice. *Atherosclerosis* 244: 179–187.
11. Pirillo, A., G.D. Norata, and A.L. Catapano. 2013. LOX-1, OxLDL, and atherosclerosis. *Mediators of Inflammation* 2013: 152786.
12. Wang, Y.J., J.T. Wang, Q.X. Fan, and J.G. Geng. 2007. Andrographolide inhibits NF-kappaBeta activation and attenuates neointimal hyperplasia in arterial restenosis. *Cell Research* 17: 933–941.
13. Ji, X., C. Li, Y. Ou, N. Li, K. Yuan, G. Yang, X. Chen, Z. Yang, B. Liu, W.W. Cheung, L. Wang, R. Huang, and T. Lan. 2016. Andrographolide ameliorates diabetic nephropathy by attenuating hyperglycemia-mediated renal oxidative stress and inflammation via Akt/NF-kappaB pathway. *Molecular and Cellular Endocrinology* 437: 268–279.
14. Lan, T., T. Wu, H. Gou, Q. Zhang, J. Li, C. Qi, X. He, P. Wu, and L. Wang. 2013. Andrographolide suppresses high glucose-induced fibronectin expression in mesangial cells via inhibiting the AP-1 pathway. *Journal of Cellular Biochemistry* 114: 2562–2568.
15. Dai, J., Y. Lin, Y. Duan, Z. Li, D. Zhou, W. Chen, L. Wang, and Q.Q. Zhang. 2017. Andrographolide inhibits angiogenesis by inhibiting the Mir-21-5p/TIMP3 signaling pathway. *International Journal of Biological Sciences* 13: 660–668.
16. Xuan, Y., Y. Gao, H. Huang, X. Wang, Y. Cai, and Q.X. Luan. 2017. Tanshinone IIA attenuates atherosclerosis in apolipoprotein E knockout mice infected with Porphyromonas gingivalis. *Inflammation* 40: 1631–1642.
17. Zhao, N., R. Wang, L. Zhou, Y. Zhu, J. Gong, and S.M. Zhuang. 2014. MicroRNA-26b suppresses the NF-kappaB signaling and enhances the chemosensitivity of hepatocellular carcinoma cells by targeting TAK1 and TAB3. *Molecular Cancer* 13: 35.
18. Ackers, I., C. Szymanski, K.J. Duckett, L.A. Consitt, M.J. Silver, and R. Malgor. 2018. Blocking Wnt5a signaling decreases CD36 expression and foam cell formation in atherosclerosis. *Cardiovascular Pathology* 34: 1–8.
19. Al, B.R., F. Al-Bayaty, M.M. Al-Obaidi, S.F. Hussain, and T.Z. Mulok. 2014. Evaluation of the effect of andrographolide on atherosclerotic rabbits induced by Porphyromonas gingivalis. *BioMed Research International* 2014: 724718.
20. Gupta, S., K.P. Mishra, S.B. Singh, and L. Ganju. 2018. Inhibitory effects of andrographolide on activated macrophages and adjuvant-induced arthritis. *Inflammopharmacology* 26: 447–456.
21. Rose-John, S. 2012. IL-6 trans-signaling via the soluble IL-6 receptor: importance for the pro-inflammatory activities of IL-6. *International Journal of Biological Sciences* 8: 1237–1247.
22. Jones, S.A., and S. Rose-John. 2002. The role of soluble receptors in cytokine biology: the agonistic properties of the sIL-6R/IL-6 complex. *Biochimica et Biophysica Acta* 1592: 251–263.
23. Li, Y., S. He, J. Tang, N. Ding, X. Chu, L. Cheng, X. Ding, T. Liang, S. Feng, S.U. Rahman, et al. 2017. Andrographolide inhibits inflammatory cytokines secretion in LPS-stimulated RAW264.7 cells through suppression of NF-kappaB/MAPK signaling pathway. *Evidence-based Complementary and Alternative Medicine* 2017: 8248142.
24. Zhu, T., D.X. Wang, W. Zhang, X.Q. Liao, X. Guan, H. Bo, J.Y. Sun, N.W. Huang, J. He, Y.K. Zhang, J. Tong, and C.Y. Li. 2013. Andrographolide protects against LPS-induced acute lung injury by inactivation of NF-kappaB. *PLoS One* 8: e56407.
25. Touyz, R.M., and A.M. Briones. 2011. Reactive oxygen species and vascular biology: implications in human hypertension. *Hypertension Research* 34: 5–14.
26. Cheng, Y.C., J.M. Sheen, W.L. Hu, and Y.C. Hung. 2017. Polyphenols and oxidative stress in atherosclerosis-related ischemic heart disease and stroke. *Oxidative Medicine and Cellular Longevity* 2017: 8526438.
27. McLaren, J.E., D.R. Michael, T.G. Ashlin, and D.P. Ramji. 2011. Cytokines, macrophage lipid metabolism and foam cells: implications for cardiovascular disease therapy. *Progress in Lipid Research* 50: 331–347.
28. Moore, K.J., F.J. Sheedy, and E.A. Fisher. 2013. Macrophages in atherosclerosis: a dynamic balance. *Nature Reviews. Immunology* 13: 709–721.
29. Kunjathoor, V.V., M. Febbraio, E.A. Podrez, K.J. Moore, L. Andersson, S. Koehn, J.S. Rhee, R. Silverstein, H.F. Hoff, and M.W. Freeman. 2002. Scavenger receptors class A-I/II and CD36 are the principal receptors responsible for the uptake of modified low density lipoprotein leading to lipid loading in macrophages. *The Journal of Biological Chemistry* 277: 49982–49988.
30. Lin, H., C. Lii, H. Chen, A. Lin, Y. Yang, and H. Chen. 2018. Andrographolide inhibits oxidized LDL-induced cholesterol accumulation and foam cell formation in macrophages. *The American Journal of Chinese Medicine* 46: 87–106.